REYNOLDS STRESS MODELS APPLIED TO CANONICAL SHOCK-TURBULENCE INTERACTION

V. Jagadish Babu and Krishnendu Sinha
Department of Aerospace Engineering
Indian Institute of Technology Bombay
Mumbai, India 400076
krish@aero.iitb.ac.in

ABSTRACT

Interaction of shock waves with turbulent flow has significant effect in high-speed flows. The shock wave amplifies the turbulent fluctuations and the amplification can be highly anisotropic. We study these aspects in the interaction of homogeneous isotropic turbulence with a normal shock wave. Existing Reynolds stress models are applied to this model problem and their accuracy is evaluated against available DNS data. We then propose an improvement to existing models to include the damping effect of unsteady shock oscillations. The modification is found to significantly improve model predictions and match DNS data over a range of Mach numbers.

1 INTRODUCTION

Shock waves present in high-speed flows can interact with turbulent boundary layers to result in high localized pressure and heat loads. Flow separation due to the adverse pressure gradient of the shock wave can be detrimental to the operation of engine intakes. Accurate numerical prediction of such flows is a challenging task, especially in the presence of strong shock waves. Several research efforts have been directed toward this goal. The interaction of turbulent fluctuations in the boundary layer with the shock wave lies at the heart of these phenomena. Shock-turbulence interaction has therefore been the focus of several studies.

Homogeneous isotropic turbulence passing through a normal shock is possibly the most fundamental shock-turbulence interaction. Compared to shock-boundary-layer interaction, the model problem does not have additional complexity due to flow separation, streamline curvature, and boundary layer velocity gradients. Shock-homogeneous turbulence interaction has been extensively studied using direct numerical simulation (DNS) (Mahesh *et al.*, 1997; Larsson & Lele, 2009). This canonical interaction is also amenable to theoretical analysis using rapid distortion theory and linear interaction analysis (Mahesh *et al.*, 1997; Durbin & Zemen, 1992; Wouchuk *et al.*, 2009). Some limited experimental data are also available (Barre *et al.*, 1996). In spite of the geometric simplicity, the model problem exhibits a range of physical effects, like generation of acoustic waves, baroclinic torques, and unsteady shock oscillations. Physical insight obtained in this canonical problem has proved useful in developing advanced turbulence models for shock-turbulence interaction (Sinha *et al.*, 2003; Sinha, 2012).

Reynolds-averaged Navier-Stokes (RANS) approach is extensively used in engineering predictions of shock/turbulent-boundary layer interaction. Conventional turbulence models like standard $k-\varepsilon$ and $k-\omega$ models predict high amplification of turbulence across the shock (Sinha *et al.*, 2003). Compressibility corrections in the form of dilatational dissipation and pressure dilatation, do not improve turbulence levels significantly. Suppressing eddy viscosity, for example by a realizable model, brings down the postshock turbulence level, but the predictions are still appreciably higher than DNS data. One of the best predictions is achieved by the shock-unsteadiness model proposed by Sinha *et al.* (2003). They have identifed a damping effect of the unsteady shock oscillations on TKE amplification and developed a model for this effect.

A key feature of shock-turbulence interaction is the anisotropy in Reynolds stresses generated downstream of the shock wave. The streamwise and transverse Reynolds stresses are amplified differently across the shock wave. An initially homogeneous isotropic disturbance field is converted into an axisymmetric turbulence and two-equation turbulence models like $k-\varepsilon$ and $k-\omega$ cannot reproduce this anisotropy in Reynolds stresses, as they model the amplification of the total effect in the form of the turbulent kinetic energy. On the other hand, models based on transport equations of individual Reynolds stresses are ideally suited to capture the anisotropic turbulence generated by the shock. Reynolds stress models (RSM) have been extensively used in low-speed flows, with some limited applications to shock-boundary layer interactions (Gerolymos *et al.*, 2004; Zha & Knight, 1996; Lee *et al.*, 1992).

The objective of the current work is to evaluate existing Reynolds stress models and propose improvements to predict the amplification of turbulence across a nominally normal shock wave. Larsson & Lele (2009) present direct numerical simulation of canonical shock turbulence interaction, where they report a range of cases for varying shock strength, turbulence intensity and Reynolds number based on Taylor microscale. The upstream turbulence field is assumed to be purely vortical with no thermodynamic fluctuations in the incoming flow. This is possibly the simplest shock-turbulence interaction, and is chosen as a starting point for studying Reynolds stress amplification. The data from these simulations is used as a benchmark for comparing different Reynolds stress models and to evaluate new physics-based models for Reynolds stresses.

2 GOVERNING EQUATIONS

In the present work, the Favre averaged Reynolds stress transport equation is adopted for compressible flow.

$$\frac{D\overline{\rho}R_{ij}}{Dt} = P_{ij} + \phi_{ij} + d_{ij} - \overline{\rho}\varepsilon_{ij} \tag{1}$$

where $R_{ij} = \widetilde{u_i''u_j''}$ is the Reynolds stress, tilde indicates Favre averaging, overbar is Reynolds averaging and double prime is Favre fluctuation. Production due to mean gradients is

$$P_{ij} = -\overline{\rho}R_{jk}\frac{\partial U_i}{\partial x_k} - \overline{\rho}R_{ik}\frac{\partial U_j}{\partial x_k},$$

ε_{ij} is the dissipation and it is assumed to be isotropic $\varepsilon_{ij} = \frac{2}{3}\varepsilon\delta_{ij}$, where ε is the turbulent dissipation rate. Direct compressiblity effects and pressure dilatation terms are neglected (Gerolymos *et al.*, 2004).

Pressure strain rate correlation (ϕ_{ij}) can be decomposed into two components namely, slow and rapid parts. The rapid term is linear in the turbulent fluctuations, and responds directly to changes in mean velocity gradient. The slow term represents turbulence-turbulence interaction. Gerolymos *et al.* (2004) computed the three dimensional shock-wave/boundary-layer interaction, by using compressible extension of Launder & Shima (1989) near-wall model. The pressure-strain correlation is modelled as,

$$\phi_{ij} = -C_1\overline{\rho}\frac{\varepsilon}{k}a_{ij} - C_2(P_{ij} - \frac{2}{3}\delta_{ij}P_k) \tag{2}$$

where, $a_{ij} = R_{ij} - \frac{2}{3}k\delta_{ij}$, $P_k = P_{ll}/2$, k is turbulent kinetic energy and constants are $C_1 = 1$, $C_2 = 0.75$ respectively. Zha & Knight (1996) used the Reynolds stress turbulence model proposed by Knight. The model is the extension of the incompressible flow model of Launder *et al.* (1975), where the pressure-strain correlation is modelled as,

$$\phi_{ij} = -C_{c1}\overline{\rho}\frac{\varepsilon}{k}a_{ij} + C_{c2}\overline{\rho}kS_{ij} \tag{3}$$

with C_{c1} = 4.3 and C_{c2}=0.17. Lee *et al.* (1992) worked on new formulation of pressure-strain and proposed a model with pressure-dilatation, the dilatation-dissipation and the mass-averaged fluctuations. As per their model,

$$\begin{aligned}\phi_{ij} =& -C_{p1}\overline{\rho}\frac{\varepsilon}{k}a_{ij} - C_{p2}(P_{ij} - \frac{2}{3}\delta_{ij}P_k) - C_3(D_{ij} - \frac{2}{3}\delta_{ij}P_k) \\ & - C_4k\overline{\rho}\left(S_{ij} - \frac{2}{3}S_{kk}\delta_{ij}\right) - C_5\overline{\rho}a_{ij} + C_6\overline{\rho}\tau_{ll}\frac{\partial U_l}{\partial x_l}\delta_{ij} \\ & + \frac{1}{3}C_7P_k\delta_{ij}\end{aligned} \tag{4}$$

where $S_{ij} = \left[\frac{\partial U_i}{\partial x_j} + \frac{\partial U_j}{\partial x_i}\right]$, $D_{ij} = -\overline{\rho}R_{ik}\frac{\partial U_k}{\partial x_j} - \overline{\rho}R_{jk}\frac{\partial U_k}{\partial x_i}$, $\tau_{ll} = R_{ll}$ and coefficient values are C_{p1} = 1.5, C_{p2}=0.76, C_3=0.10, C_4=0.18, C_5=0.14, C_6=0.35 respectively.
The transport equation for the turbulence dissipation rate is

$$\frac{D\overline{\rho}\varepsilon}{Dt} = -C_{\varepsilon1}\overline{\rho}R_{ij}\frac{\varepsilon}{k}\frac{\partial U_i}{\partial x_j} - C_{\varepsilon2}\overline{\rho}\frac{\varepsilon^2}{k} \tag{5}$$

where constants are $C_{\varepsilon1}$ = 1.44, $C_{\varepsilon2}$ = 1.92, from Gerolymos *et al.* (2004).

Note that diffusion terms are not include in Eqs. 1 and 5 as they are found to have a small effect in the region of the shock wave

2.1 Simplification for Canonical Shock-Turbulence Interaction

For homogeneuos isotropic turbulence passing through a normal shock, the transport equations for the Reynolds stresses simplify to a one-dimensional form. For Gerolymos and Vallet (GV) model, the equations for the axial (shock-normal) component R_{11} and the transverse (shock parallel) component R_{22} are given by

$$U\frac{\partial R_{11}}{\partial x} = (-2 + \frac{4}{3}C_2)R_{11}\frac{\partial U}{\partial x} - C_1\varepsilon a_{11} - \frac{2}{3}\varepsilon \tag{6}$$

$$U\frac{\partial R_{22}}{\partial x} = -\frac{2}{3}C_2(R_{11}\frac{\partial U}{\partial x}) - C_1\varepsilon a_{22} - \frac{2}{3}\varepsilon \tag{7}$$

For Zha & Knight (1996) model, the equations for R_{11} and R_{22} simplify to

$$U\frac{\partial R_{11}}{\partial x} = (-2R_{11} + C_{c2}(R_{11} + 2R_{22}))\frac{\partial U}{\partial x} - C_{c1}\varepsilon a_{11} - \frac{2}{3}\varepsilon \tag{8}$$

$$U\frac{\partial R_{22}}{\partial x} = -C_{c1}\varepsilon a_{22} - \frac{2}{3}\varepsilon \tag{9}$$

For Lee *et al.* (1992) model, the equations are given by

$$U\frac{\partial R_{11}}{\partial x} = (-2 + A')R_{11}\frac{\partial U}{\partial x} + B'R_{22}\frac{\partial U}{\partial x} - C_{p1}\varepsilon a_{11} - \frac{2}{3}\varepsilon \tag{10}$$

$$U\frac{\partial R_{22}}{\partial x} = C'R_{11}\frac{\partial U}{\partial x} + D'R_{22}\frac{\partial U}{\partial x} - C_{p1}\varepsilon a_{22} - \frac{2}{3}\varepsilon \tag{11}$$

$$\begin{aligned}A' &= \left(\frac{4}{3}C_{p2} + \frac{4}{3}C_3 - \frac{2}{3}C_4 - \frac{2}{3}C_5 + C_6\right) \\ B' &= \left(\frac{2}{3}C_5 - \frac{4}{3}C_4\right) \\ C' &= \left(-\frac{2}{3}C_{p2} - \frac{2}{3}C_3 + \frac{1}{3}C_4 + \frac{1}{3}C_5 + C_6\right) \\ D' &= \left(\frac{2}{3}C_4 - \frac{1}{3}C_5\right)\end{aligned} \tag{12}$$

Here, x is the shock normal direction, U is the mean velocity in the x-direction and the equation for R_{33} is identical to that of R_{22}.

3 MODEL EVALUATION

Larsson & Lele (2009) present direct numerical simulation (DNS) of the interaction of the homogeneous isotropic turbulence with a normal shock for Mach number varying from 1.27 to 6. Turbulent Mach number in the range 0.15-0.22 at Reynolds number based on taylor microscale, Re_λ = 40 are consider in the current study and are used to specify initial and boundary conditions for the Reynolds stress equations.

Sinha & Balasridhar (2013) show that turbulent dissipation has negligible effect at the shock, and can be neglected. Same is true for the slow part of the pressure strain term that is proportional to the dissipation rate ε. Eqs. 6 and 7 can thus be analytically integrated across the shock to get

$$\frac{R_{11d}}{R_{11u}} = \left[\frac{U_u}{U_d}\right]^{2-\frac{4}{3}C_2} \tag{13}$$

$$\frac{R_{22d}}{R_{22u}} = 1 + \frac{2}{3}C_2\left[\frac{U_u - U_d}{U_d}\right] \tag{14}$$

For Zha & Knight (1996), transverse Reynolds stress remains constant through the shock and the shock-normal Reynolds stress is given by

$$U\frac{\partial R_{11}}{\partial x} = (-2R_{11} + C_{c2}(R_{11} + 2R_{22}))\frac{\partial U}{\partial x} \tag{15}$$

For Lee *et al.* (1992)

$$U\frac{\partial R_{11}}{\partial x} = AR_{11}\frac{\partial U}{\partial x} + BR_{22}\frac{\partial U}{\partial x} \tag{16}$$

$$U\frac{\partial R_{22}}{\partial x} = CR_{11}\frac{\partial U}{\partial x} + DR_{22}\frac{\partial U}{\partial x} \tag{17}$$

where constants are A=-0.70, B=-0.14, C=-0.12, D=0.07.

Here, 13 and 14 equations are integrated analytically, whereas 15, 16, 17 equations are integrated numerically for a specified mean flow profile across the shock wave. The amplification of the Reynolds stresses for varying Mach number from different models are plotted in Fig. 1 for axial and transverse components. Zha & Knight (1996) model predicts very high amplification for all Mach numbers. Gerolymos *et al.* (2004) model and Lee *et al.* (1992) model have good match for lower Mach numbers upto 1.5, beyond which they over predict the DNS data for R_{11}. The amplification of the transverse Reynolds stress is lower than that of R_{11}, as per DNS and the model equations. The R_{22} trends for Gerolymos *et al.* (2004) model and Lee *et al.* (1992) models are similar to that of R_{11}, whereas Zha & Knight (1996) model yields no R_{22} amplification for all Mach numbers.

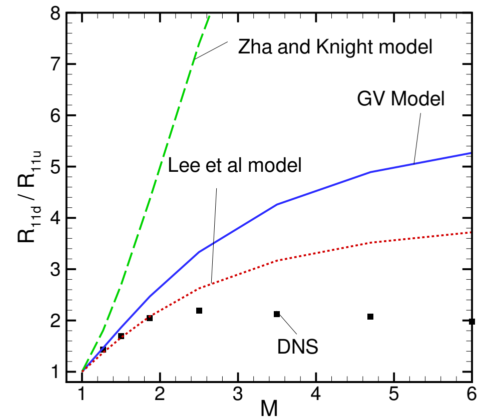

(a)

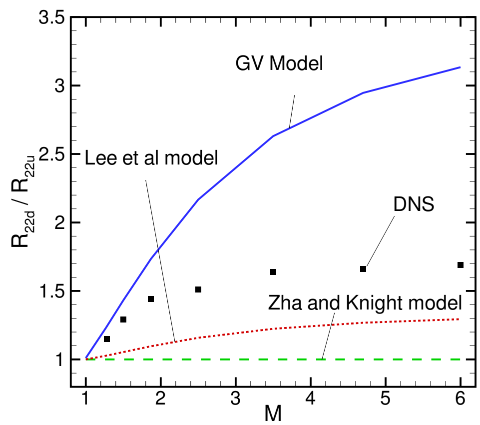

(b)

Figure 1: Reynolds stress amplification in a shock/turbulence interaction as a function of upstream Mach number for different RSM compared with DNS data

4 MODEL IMPROVEMENTS

Sinha *et al.* (2003) use linear interaction analysis (LIA) to study the amplification of turbulent kinetic energy in a canonical shock-turbulence interaction. In this approach, the inviscid shock wave is treated as a discontinuity and the upstream turbulence field is decomposed into Fourier modes. Elementary interaction of a two-dimensional single wave with the deformed and unsteady shock wave forms the heart of this theory. For a given upstream Mach number and plane wave incidence angle, the theory predicts the disturbance waves generated downstream of the shock. A superposition of the two-dimensional results for a specified upstream energy spectrum yields the downstream statistics for three-dimensional turbulence. Comparison with available DNS data yield good match for the amplification of turbulent kinetic energy and its dissipation rate across the shock wave (Sinha *et al.*, 2003; Larsson & Lele, 2009; Sinha, 2012).

Sinha *et al.* (2003) linearize the governing equations about the unsteady distorted shock wave, and use them to derive transport equations for the normal Reynolds stresses. It is based on the assumption that the turbulent fluctuations are small compared to the jump in the mean flow quantities across the shock. They also compute a budget of the different source terms across the shock using LIA data. It is found that the amplification of turbulent kinetic energy is primarily due to the production by mean dilatation. There is an additional source term representing the effect of shock-unsteadiness on the shock-normal Reynolds stress component. This damping term is of the form $\widetilde{u''\xi_t}\partial U/\partial x$ and is responsible for the reduction in TKE amplification at the shock. Here, $x = \xi(y,z,t)$ is the deviation of the shock wave from its mean location of $x = 0$. The temporal derivative ξ_t thus represents the instantaneous speed of the shock wave.

The correlation $\widetilde{u''\xi_t}$ represents a coupling between the unsteady shock motion and the turbulent velocity fluctuations in the streamwise direction. Sinha *et al.* (2003) propose a model for the unclosed correlation.

$$\widetilde{u''\xi_t} = b_1' R_{11} \tag{18}$$

based on the assumption that the shock unsteadiness is primarily caused by the incoming turbulent fluctuations. LIA results are used to obtain the model coefficient

$$b_1' = 0.4\left(1 - e^{1-M_1}\right) \tag{19}$$

as a function of the upstream mean flow Mach number. The resulting model equation, including the shock-unsteadiness damping term, yields a significant improvement over existing models. It is found to match DNS data for the amplification of turbulent kinetic energy across a range of Mach numbers.

In the present work, we apply the shock-unsteadiness damping term to the Reynolds stress model of Gerolymos *et al.* (2004). The modified R_{11}-equation takes the form

$$U\frac{\partial R_{11}}{\partial x} = (-2 + 2b_1' + \frac{4}{3}C_2)R_{11}\frac{\partial U}{\partial x} - C_{c1}\varepsilon a_{11} - \frac{2}{3}\varepsilon \tag{20}$$

and the R_{22}- and ε-equation remain unchanged. The amplification of R_{11} and R_{22} across the shock are thus given by

$$\frac{R_{11d}}{R_{11u}} = \left[\frac{U_u}{U_d}\right]^{2(1-b_1')-\frac{4}{3}C_2} \tag{21}$$

$$\frac{R_{22d}}{R_{22u}} = 1 + \frac{2}{3}C_2\left[\frac{U_u^{(1-2b_1')} - U_d^{(1-2b_1')}}{(1-2b_1')U_d^{(1-2b_1')}}\right] \tag{22}$$

and are plotted in Fig. 2 as a function of upstream Mach number. It is found that the new model significantly reduces the post-shock Reynolds stresses. However, it predicts too low a value of post-shock R_{11} for higher Mach numbers, R_{22} amplification is over-predicted for strong shocks. Note that the model constant C_2 is taken to be 0.75 as proposed by Gerolymos and Vallet to incorporate near-wall effects. By comparison, Launder & Shima (1989) propose a value

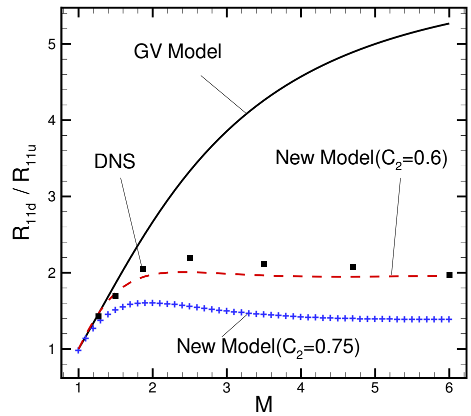

(a)

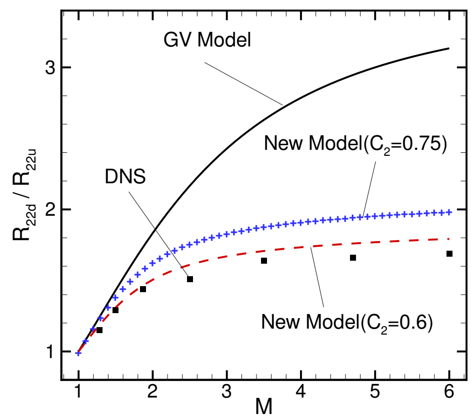

(b)

Figure 2: Effect of model improvements on Reynolds stress amplification across a normal shock at various Mach numbers

of $C_2 = 0.6$ for the rapid pressure strain term in isotropic turbulence. Changing the model constant C_2 from 0.75 to 0.6 improve the predictions considerably (see Fig. 2). A lower value of C_2 leads to a higher amplification of R_{11} and it is close to the DNS data reported by Larsson & Lele (2009). Reducing C_2 also leads to a close comparison with the DNS data for R_{22} amplification across the shock wave.

Next, we study the variation of the Reynolds stresses as a function of the streamwise distance from the shock wave. The model predictions for R_{11} and R_{22} are plotted along with DNS data in Figs. 3 and 4 respectively. The DNS data shows large values of R_{11} near the shock (at $x = 0$) and a rapid non-monotonic variation immediately downstream ($x \leq 3$). The shock-unsteadiness model does not predict these phenomena, but accounts for their net effect on the turbulence amplification. We therefore extrapolate the downstream decay of R_{11} back to the shock location (shown by open squares in Fig. 3) and compare these with the model prediction.

Similarly, R_{22} shows a sharp peak immediately behind the shock, once again due to acoustic transient phenom-

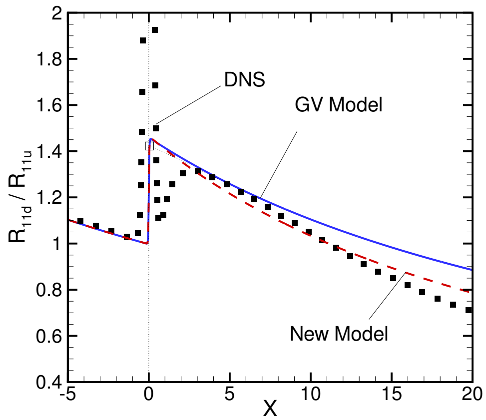

(a)

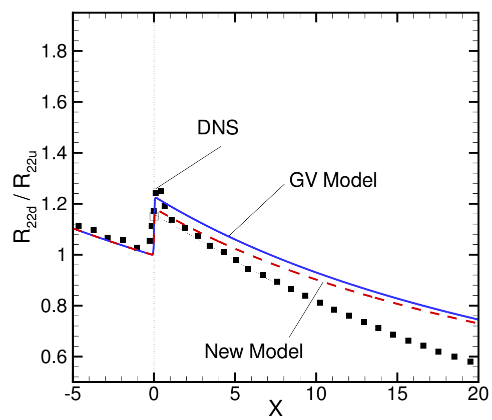

(a)

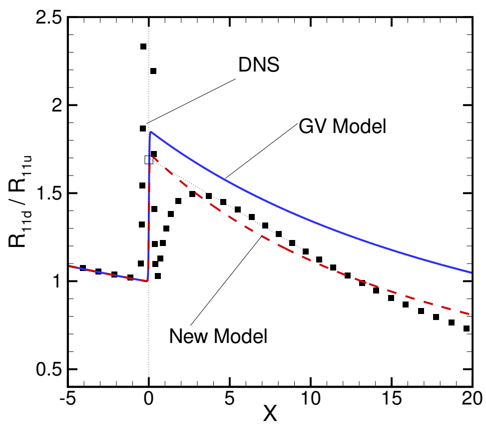

(b)

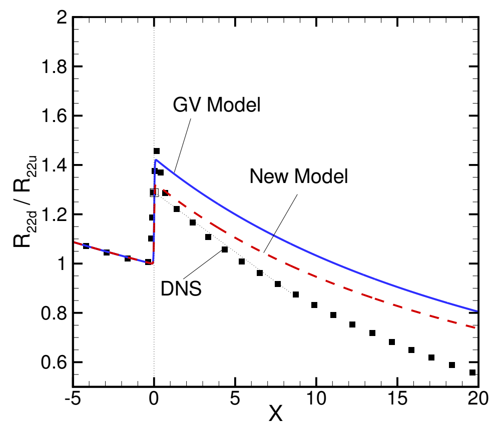

(b)

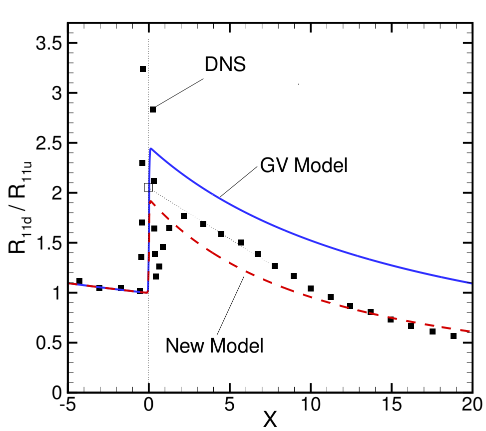

(c)

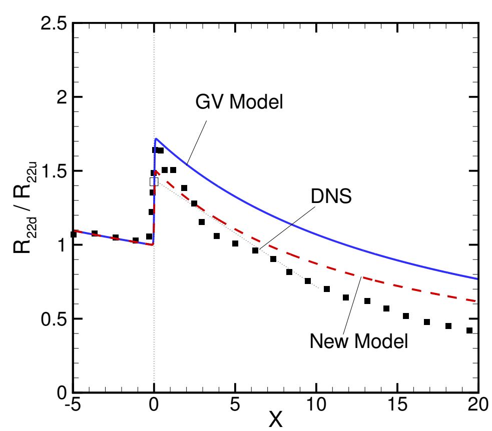

(c)

Figure 3: Streamwise evolution of R_{11} for homogenenous isotropic turbulence interacting with normal shock at (a) 1.27, (b) 1.5, (c) 1.87.

Figure 4: Streamwise evolution of R_{22} for homogenenous isotropic turbulence interacting with normal shock at (a) 1.27, (b) 1.5, (c) 1.87.

ena. The shock-extrapolated values of R_{22} (shown in Fig. 4) without the transient peak are compared with model predictions.

The Reynolds stresses show a monotonic decay upstream of the shock, up to a normalized value of 1. The models predict a jump in R_{11} and R_{22} at the shock followed by another decay with downstream distance. Both GV model and the new model with shock-unsteadiness correction match the extrapolated DNS jump in R_{11} for the Mach 1.27 case in Fig. 3a. The new model predicts the jump correctly for the Mach 1.5 shock wave and slightly underpredicts the DNS jump at Mach 1.87.

The downstream decay of R_{11} is determined by its dissipation rate ε_{11}, which is governed by the corresponding transport equation (1). The model coefficient $C_{\varepsilon 1}$ is set to 1.44 in the GV model, whereas a slightly higher value of 1.7 is found to match the decay in DNS data.

Further, the isotropic assumption for the dissipation rate is replaced by

$$\varepsilon_{ij} = \frac{R_{ij}}{k}\varepsilon \tag{23}$$

to bring in the anisotropy effects in the post-shock flow. The anisotropy factor is taken from DNS data of Larsson *et al*. and a typical value of 1.3 is used (see Fig. 4c in Larsson & Lele (2009)). We thus get $\varepsilon_{11} = 0.78\varepsilon$ and $\varepsilon_{22} = 0.6\varepsilon$ and the downstream decay is reproduced well for Mach 1.27 and 1.5 shock waves. For the Mach 1.87 the new model underpredicts the post-shock R_{11} values for up to $x = 10$ but is comparable to the DNS data beyond that. Overall, the proposed model with shock-unsteadiness correction shows appreciable improvement over the original model proposed by Gerolymos *et al.* (2004).

For the transverse Reynolds stress R_{22}, both GV model and the shock-unsteadiness model give comparable results at low Mach numbers (Fig. 4a). They reproduce the DNS jump well, but over-predict the downstream value considerably. For higher Mach numbers, the GV model appears to be closer to the peak R_{22} value at the shock, but the new model reproduces the jump in R_{22} without the transient peak. Overall, the new model is closer to the DNS data than the GV model; both give a slower decay of the transverse Reynolds stress behind the shock wave. Note that the comparisons shown in Figs. 3 and 4 are at relatively low supersonic Mach numbers, but the trend is expected to be similar for stronger shock waves as well.

5 CONCLUSION

In this paper, we apply existing Reynolds stress models to the interaction of homogeneous isotropic turburlence with a nominally normal shock wave. The governing equations are simplified for one-dimensional mean, and integrated to yield the jump in the normal Reynolds stresses across the shock. Comparison with available DNS data shows significant over prediction, especially at high Mach numbers. A modification is proposed based on linear inviscid theory applied to shock-turbulence interaction. The damping effect of unsteady shock motion is included in the transport equation, and the shock-unsteadiness parameter is taken from previous studies based on linear interaction analysis. It is found to significantly improve the model predictions, and the amplification across the shock compares well with DNS data over a large range of Mach numbers. Additional modifications to the closure coefficients are proposed to match the DNS decay of Reynolds stresses downstream of the shock wave.

REFERENCES

Barre, S., Alem, D. & Bonnet, J. P. 1996 Experimental Study of a Normal Shock / Homogeneous Turbulence Interaction. *AIAA Journal* **34** (5), 968–974.

Durbin, P. A. & Zemen, O. 1992 Rapid distortion theory for homogeneous compressed turbulence with application to modelling. *J. Fluid Mech.* **242**, 349–370.

Gerolymos, G. A., Sauret, E. & Vallet, I 2004 Oblique-Shock-Wave/Boundary-Layer Interaction Using Near-Wall Reynolds Stress Models. *AIAA Journal* **42** (6), 1089–1100.

Larsson, J. & Lele, S. K. 2009 Direct numerical simulation of canonical shock / turbulence interaction. *Physics of Fluids* **21**, 126101.

Launder, B. E., Reece, G. J. & Rodi, W. 1975 Progress in the development of a Reynolds-stress turbulence closure. *Journal of Fluid Mechanics* **68** (03), 537–566.

Launder, B. E. & Shima, N. 1989 Second-Moment Closure for the Near-Wall Sublayer : Development and Application. *AIAA Journal* **27** (10), 1319–1325.

Lee, J., Taulbee, D. B. & Holden, M. S. 1992 Study of Turbulence on Supersonic Compression Surfaces Using Reynolds Stress Model. *AIAA Journal* **30** (7), 1738–1746.

Mahesh, K., Lele, S. K. & Moin, P. 1997 The influence of entropy fluctuations on the interaction of turbulence with a shock wave. *Journal of Fluid Mechanics* **334**, 353–379.

Sinha, K. 2012 Evolution of enstrophy in shock/homogeneous turbulence interaction. *Journal of Fluid Mechanics* **707**, 74–110.

Sinha, K. & Balasridhar, S. J. 2013 Conservative Formulation of the k - ε Turbulence Model for Shock-Turbulence Interaction. *AIAA Journal* **51** (8).

Sinha, K., Mahesh, K. & Candler, G. V. 2003 Modeling shock unsteadiness in shock/turbulence interaction. *Physics of Fluids* **15** (8), 2290.

Wouchuk, J., Huete Ruiz de Lira, C. & Velikovich, A. 2009 Analytical linear theory for the interaction of a planar shock wave with an isotropic turbulent vorticity field. *Physics Review E* **79**, 066315.

Zha, Ge-cheng & Knight, Doyle 1996 Three-Dimensional Shock / Boundary-Layer Interaction Using Reynolds Stress Equation Turbulence Model. *AIAA Journal* **34** (7), 1313–1320.